

THERMO-EMFS OF BINARY TRANSITION-METAL SOLID
SOLUTIONS CONTAINING ISOELECTRONIC COMPONENTS

V. V. Artishevskaya and Yu. P. Zarichnyak

UDC 537.322+669.295

An approximate method is given for calculating the thermo-emf of an alloy.

Formulation. The current theory of thermoelectric parameters does not at present provide a rigorous analytic method of forecasting thermo-emf for alloys whose components form binary disordered continuous solid solutions with an error comparable with the error of measurement [1-3].

It is necessary to synthesize materials with preset properties, so one needs approximate analytic methods that can employ a minimal volume of input data such as the properties α_1 and α_2 of the components and one value for the property of the alloy $\alpha_{12}(\tilde{x})$ of known composition \tilde{x} in order to forecast the thermo-emf and the composition dependence at the development stage:

$$\alpha_{12}(x) = f(\alpha_1, \alpha_2, \alpha_{12}(\tilde{x}), x)$$

throughout the component concentration range.

The prospects for this approach are confirmed by papers on the electrical, mechanical, and thermophysical parameters of alloys and composites containing various substances [2-9].

The phenomenological equations of nonequilibrium thermodynamics have been used [2, 3] to show that the thermo-emf and the concentration dependence are related to characteristics such as the thermal and electrical conductivities.

An approximate method for these alloys can be based on the theory of generalized conductivity [4, 5], where the methods have been developed for thermo-emf [3], resistivity, and thermal conductivity of solid solutions with continuous or restricted solubility and containing two or more components [5-9]. In [1], there are systematic measurements on resistivity and thermo-emf for these binary alloys.

Classification of Binary Continuous Solid Solutions and Structure Analysis. The classification of [1] indicates that all these binary continuous solid solutions (BCSS) can be divided into two main types in accordance with the common features in the electronic structures of the components. All the components of BCSS that form systems of type I are isoelectronic elements in the same group in the periodic system; ones consisting of other components belong to type II.

Here we consider a method for calculating (forecasting) the dependence of the thermo-emf α on composition x for type I. Two forms may occur (Fig. 1). Usually, $\alpha(x)$ is a smooth curve convex towards the composition axis (curve 1 in Fig. 1). We assign this as group IA. However, $\alpha(x)$ may not have a turning point (curve 2 in Fig. 1, group IB). It is considered [1] that type I is characteristic of isoelectronic metals with small differences in atomic mass. The minimum thermo-emf for IA corresponds to equal atomic (molar) component concentrations, and the same applies to a certain mean value (in relation to the properties of the components) for IB.

We consider the structure at the microscopic level. The B atoms with the lower concentration ($x_B < 50$) will be called those of the minor component, and they enter the lattice of the main component A ($x_A > 50$) and cause certain distortions in the electronic and lattice structures in regions of finite size around them (perturbation zone), so the properties are altered in that zone, $\alpha_{AB} \neq \alpha_A, \alpha_B$. As A and B and these zones are thermoelectrically

Leningrad Fine Mechanics and Optics Institute. Translated from *Inzhenerno-Fizicheskii Zhurnal*, Vol. 53, No. 2, pp. 275-280, August, 1987. Original article submitted May 19, 1986.

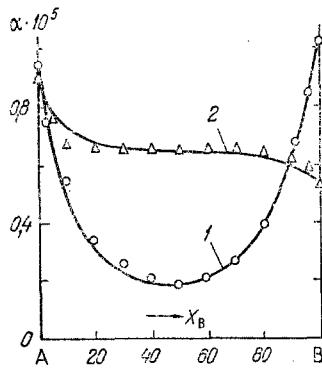


Fig. 1

Fig. 1. Behavior of thermo-emf for binary continuous solid solutions: the lines are by calculation from the proposed method and the points are from experiment [1]: 1) titanium-zirconium alloys; 2) titanium-hafnium.

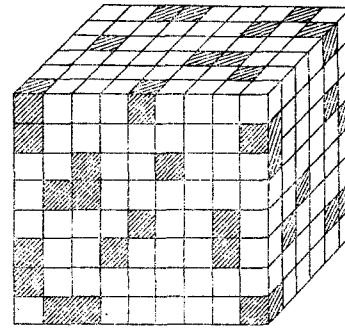


Fig. 2

Fig. 2. Structure of the solution as a random mixture of perturbation zones and the main component.

inhomogeneous, $\alpha_A \neq \alpha_B$, one gets circulating microcurrents in the solid solution and local temperature gradients. These inhomogeneities increase the entropy [2] and the carrier scattering as well as the thermal energy [2, 5-9]. These zones are assumed to be randomly distributed in the disordered solution. The treatment can be simplified [6-9] by representing the structure for the range $0 < x_B < 50$ as a mixture at the microscopic level consisting of component A (component 1) unperturbed by B and volumes containing the AB perturbation zones around the B atoms, where there are altered parameters α_{AB} (component 2). Here α_{AB} is taken as equal to the thermo-emf of a solid solution with equiatomic concentrations, $\alpha_{AB} = \alpha(x_A = x_B = 50)$, which is known from experiment. If $\alpha(x_A = x_B)$ is unknown but a value is available for $\alpha(x_A \neq x_B)$, one can calculate $\alpha(x_A = x_B)$ from $\alpha(x_A \neq x_B)$ via the recommendations of [8]. In the range $50 < x_B < 100$, the structure is considered as a mixture at the microscopic level of components AB and B; the two microheterogeneous subsystems A + AB and AB + B thus amount to disordered mixtures with given properties for the components α_A and α_{AB} , α_{AB} and α_B . The volume concentration of the components in the A + AB, AB + B subsystems, i.e., the volume concentration v_{AB} of the perturbed zones, is proportional to the minor-component concentration, $v_{AB} \sim f(x)$, but the relationship is somewhat more complicated than linear [6, 8].

We represent the structure as a combination of two binary mixtures (subsystems A + AB, AB + B) [6] to calculate the properties by means of well-developed methods for simulating mixture structures and by using methods for calculating properties approximately at the macroscopic level [5] and the microscopic one [5-9].

We calculate v_{AB} from approximate formulas used repeatedly in [6-9]:

$$v_{AB} = \frac{x}{100} [1 + N(x)], \quad (1)$$

$$N(x) = 6 \exp[-14,334 \cdot 10^{-4} x^2 (1 - 0,001x)] - 0,315x(0,5 - 0,01x)^2, \quad (2)$$

where

$$x = \begin{cases} x_B & \text{for } 0 < x_B < 50, \\ 100 - x_B & \text{for } 50 < x_B < 100. \end{cases}$$

One can calculate the thermo-emf of the solid solution from the properties of the subsystem components α_A , α_{AB} and α_B , α_{AB} and the volume concentration $v_{AB}(x)$.

Calculating BCSS Thermo-emf. We selected a model adequately reflecting the structure as a three-dimensional system of close-packed cubic cells, with part of the volume filled by A (open cubes, $0 < x_B < 50$), while the hatched cubes simulate the randomly disposed perturbation zones. For $x_B > 50$ the light cubes are filled with component B.

The differences in component properties (α_{AB}/α_A , α_{AB}/α_B) mean that one should use various simplified models to calculate the effective thermo-emfs for the subsystems (Fig. 2).

If $0.01 < (\alpha_{AB}/\alpha_A, \alpha_{AB}/\alpha_B) < 100$, with an error $(\Delta\alpha/\alpha) \leq 10\%$ comparable with the spread in the reference data on α_A , α_B , λ_A , λ_B , ρ_A , ρ_B and α_{AB} , λ_{AB} , ρ_{AB} from different sources one can use an ordered model with interpenetrating components [10].

For that structure

$$\alpha = \left[\alpha_1 c^2 + \alpha_2 (1-c)^2 \frac{\rho_1}{\rho_2} + 2\alpha_{12} \frac{\rho_1}{\rho_{12}} c(1-c) \right] \frac{\rho}{\rho_1}, \quad (3)$$

$$\rho = \rho_1 \left[c^2 + (1-c)^2 \frac{\rho_2}{\rho_1} + 2c(1-c) \frac{\rho_1}{\rho_{12}} \right]^{-1}, \quad (4)$$

$$\rho_{12} = c\rho_1 + (1-c)\rho_2 + \frac{c(1-c)(\alpha_1 - \alpha_2)^2 T}{\lambda_1(1-c) + \lambda_2 c}, \quad (5)$$

$$\text{for } 0 < x_B \leq 50 \quad \alpha_1 = \alpha_A, \rho_1 = \rho_A, \lambda_1 = \lambda_A, \lambda_2 = \lambda_{AB} \quad (\tilde{x} = x_B = 50),$$

$$\alpha_2 = \alpha_{AB} \quad (\tilde{x} = x_B = 50), \quad \rho_2 = \rho_{AB} \quad (\tilde{x} = x_B = 50);$$

$$\text{for } 50 < x_B < 100 \quad \alpha_1 = \alpha_B, \rho_1 = \rho_B, \lambda_1 = \lambda_B, \alpha_2 = \alpha_{AB} \quad (\tilde{x} = x_B = 50),$$

$$\lambda_2 = \lambda_{AB} \quad (\tilde{x} = x_B = 50), \quad \rho_2 = \rho_{AB} \quad (\tilde{x} = x_B = 50),$$

$$\alpha_{12} = [\alpha_1 c v_\lambda + \alpha_2 (1-c)] / [1 - (1 - v_\lambda) c], \quad v_\lambda = \lambda_2 / \lambda_1.$$

Parameter c is related to v_{AB} by

$$2c^3 - 3c^2 + 1 = v_{AB}. \quad (6)$$

The solution to (6) is

$$c = 0.5 + A \cos \frac{\varphi}{3}, \quad 270 \leq \varphi \leq 360, \quad (7)$$

$$\text{for } 0 < v_{AB} \leq 0.5 \quad A = -1, \quad \varphi = \arccos(1 - 2v_{AB});$$

$$\text{for } 0.5 < v_{AB} < 1.0 \quad A = 1, \quad \varphi = \arccos(2v_{AB} - 1).$$

Components 1 and 2 in (2)-(7) are A and AB for $0 < x_B < 50$ or AB and B for $50 < x_B < 100$. For $x_B > 50$, A is the minor component, which involves corresponding changes in the subscripts when (1) and (2) are used.

Method Test and Comparison with Experiment. Measurements were compared with calculations for titanium-zirconium alloys (type IA) and titanium-hafnium ones (type IB) to test the method (Fig. 1). The calculated values agree qualitatively and quantitatively with the measurements throughout the concentration ranges; the discrepancies are usually less than 10%.

If the subsystem component properties differ more substantially, this method can be used as a first approximation.

A second approximation can be based on combining the theory of generalized conductivity with percolation theory [11]; instead of a simplified model for a two-level layer, one can use some more complicated models for percolation structures [11], which correspondingly complicates the algorithm.

The titanium-hafnium system has no turning point in $\alpha(x)$, which distinguishes it from other such systems with isoelectronic components [1]. Other kinetic coefficients are the thermal conductivity λ [6] and the electrical conductivity σ [1], which are related to α by [2]

$$\lambda = \delta - \alpha^2 \sigma T \quad (8)$$

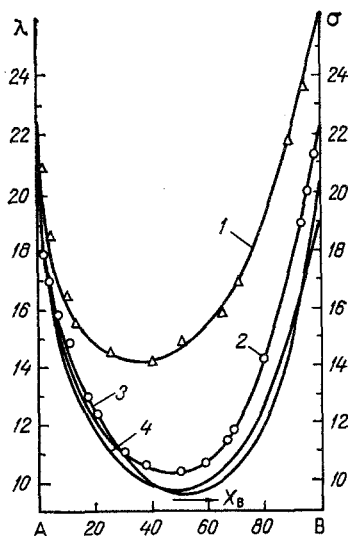


Fig. 3. Behavior of the thermal and electrical conductivities of binary continuous solid solutions (from experiment); thermal conductivity [7]: 1) titanium-zirconium; 2) titanium-hafnium, $T = 293^\circ\text{K}$; electrical conductivity [1]: 3) titanium-zirconium; 4) titanium-hafnium, $T = 298^\circ\text{K}$.

where δ is a factor relating the heat flux and the temperature-gradient pattern [2] in the kinetic equation for the entropy flux; these quantities vary in accordance with (8) and give concentration-dependence curves convex towards the composition axis and with minima near $x_A = x_B = 50$ (Fig. 3).

All three components of the binary alloys lie in a single vertical column in the periodic table and are similar in structure not only in the outer valency shell but also in the previous ones ($3d^24s^2$ for titanium, $4d^25s^2$ for zirconium, and $5d^26s^2$ for hafnium), while they belong to the same group of metals of the first type (A metals) in the classification of [12].

If the measurements of [1] are correct (there appear to be some possible sources distortion), this feature in $\alpha(x)$ for these alloys of types IA and IB (curves 1 and 2 in Fig. 1) may be examined in future research. We therefore have to consider whether this discrepancy in the forms of $\alpha(x)$, $\lambda(x)$, and $\sigma(x)$ is unique amongst such systems [1]. This appears not to be so, since a subsequent paper from the same source [13] shows that the molybdenum-vanadium system shows such features in $\alpha(x)$ and $\sigma(x)$, where analogous continuous solutions are formed. The $\alpha(x)$ and $\sigma(x)$ curves have minima for 4, 293, and 700°K and are convex towards the composition axis. However, at 1000, 1300, and 1500°K , the turning point in $\sigma(x)$ is replaced by a monotone curve, while $\alpha(x)$ retains a minimum near the equiatomic concentration. Molybdenum and vanadium lie in different columns and correspondingly differ in shell structure ($3d^34s^2$ for vanadium and $4d^55s^1$ for molybdenum). These features [1, 13] of $\alpha(x)$ and $\sigma(x)$ are of interest to further research.

Our method enables one to forecast the thermo-emf of such an alloy for the different types (IA and IB) as well as $\alpha(x)$ at the stage of development, and it enables one to evaluate the scales of the effects from the definitive parameters and provides an optimum program for measurements on synthetic materials, where one can analyze and fit the measurements.

NOTATION

$\alpha_1, \alpha_2, \alpha_3$, thermo-emfs of components and of equiatomic alloy ($X_A = X_B = 50$ at. %), V/K; x_i , component concentrations in at. % ($i = A$ or B , where A represents the main component, $x > 50$ at. %, and B is the minor component, $x < 50$ at. %); $\alpha_A, \alpha_B, \alpha_{AB}$, thermo-emfs of main component, minor component, and perturbation zones, V/K; v_{AB} , volume concentration of perturbation zone; N , coordination number.

LITERATURE CITED

1. M. V. Vedernikov, V. G. Dvunitkin, and A. Zhumagulov, *Fiz. Tverd. Tela*, 20, No. 11, 3302-3305 (1978).
2. I. I. Novikov, *Surveys on the Thermophysical Properties of Substances* [in Russian], No. 3, Moscow (1977), pp. 3-42.
3. I. I. Novikov, *Surveys on the Thermophysical Properties of Substances* [in Russian], No. 1, Moscow (1980), pp. 9-36.
4. G. N. Dul'nev and V. V. Novikov, *Inzh.-Fiz. Zh.*, 33, No. 3, 439-443 (1977).
5. G. N. Dul'nev and Yu. P. Zarichnyak, *Forecasting the Thermophysical, Electrophysical, and Physicomechanical Properties of Mixtures and Composites: Preprint of a Paper at the Fifth European Conference on the Thermophysical Properties of Solids* [in Russian], Moscow (1976).
6. Yu. P. Zarichnyak and T. A. Lisnenko, *Inzh.-Fiz. Zh.*, 33, No. 4, 642-647 (1977).
7. E. M. Savitskii, V. F. Terekhova, Yu. P. Zarichnyak, et al., *Proceedings of the Third All-Union Conference on Alloys of Rare and Refractory Metals Having Special Physical Properties* [in Russian], Moscow (1979), pp. 134-136.
8. V. F. Glushkova, Yu. P. Zarichnyak, T. A. Lisnenko, and P. A. Tikhonov, *A Study of the Properties of Solid Solutions of Rare-Earth Oxides* [in Russian], Moscow (1977), Dep. VINITI, No. 2963-77.
9. A. A. Basov, Yu. P. Zarichnyak, and T. A. Lisnenko, *Teplofiz. Vys. Temp.*, 15, No. 4, 918-926 (1977).
10. G. N. Dul'nev, *Inzh.-Fiz. Zh.*, 9, No. 3, 399-404 (1965).
11. D. P. Volkov, G. N. Dul'nev, Yu. P. Zarichnyak, and B. L. Muratova, *Inzh.-Fiz. Zh.*, 46, No. 2, 247-252 (1984).
12. G. Schulze, *Metal Physics* [Russian translation], Moscow (1971).
13. A. Zhumagulov and M. V. Vedernikov, *Fiz. Tverd. Tela*, 22, 892-894 (1980).

PARAMETERS OF A COUNTERCURRENT THERMAL-DIFFUSION
APPARATUS WITH FLOW CLOSURE AND SAMPLING

G. D. Rabinovich and A. V. Suvorov

UDC 621.039.341.6

Formulas have been derived for the optimum apparatus parameters.

An apparatus has been described [1] based on a planar thermal-diffusion column, with the mixture pumped in opposite directions at the ends. A closed loop can be used (Fig. 1b) or partial or complete product tapoff (Fig. 1a and c). The apparatus and the calculation method [2] were devised for separating petroleum oil fractions. One can evaluate the performance in separating other liquid or gas mixtures under laboratory or plant conditions by means of a more general method, which has been used in considering apparatus with complete product removal (Fig. 1c) [3, 4] or with complete product return (Fig. 1b) [5]. Our purpose is a theoretical analysis of the case where part of the material is returned (Fig. 1a).

We consider the stationary separation of a binary liquid mixture, where the concentration changes occur in the range allowing of the approximation $c(1-c) \approx a + bc$, which includes important cases such as removing a minor impurity when the content of the main component is high ($c(1-c) \approx 1-c$) and enrichment when there is only a low content of the main component ($c(1-c) \approx c$). The model [3-5] shows that the target component passes through the separating region:

$$\tau = H \left[a + bc - \frac{dc}{dy} \right], \quad (1)$$

Lykov Institute of Heat and Mass Transfer, Academy of Sciences of the Belorussian SSR, Minsk. Translated from *Inzhenerno-Fizicheskii Zhurnal*, Vol. 53, No. 2, pp. 280-284, August, 1987. Original article submitted May 10, 1986.